Available online at www.sciencedirect.com

ScienceDirect

Ceramics International 40 (2014) 123–128

CERAMICS INTERNATIONAL

www.elsevier.com/locate/ceramint

Shear-rate dependence modeling of gelcast slurries: Effects of dispersant content and solid loading

A. Nojoomi*, M.A. Faghihi-Sani, M. Khoshkalam

Department of Materials Science and Engineering, Sharif University of Technology, P.O. Box 11365-9466, Tehran, Iran

Received 6 April 2013; received in revised form 17 May 2013; accepted 29 May 2013
Available online 14 June 2013

Abstract

Gelcasting, as a ceramic forming technique, is getting worldwide attention, in that it can be used to make high-quality, complex-shaped ceramic parts with a wide range of powders. However, a model, which can appropriately describe the shear rate dependence behavior of the slurry in casting process simulation, is limited. Therefore, this study mainly sought to investigate the best model representing the behavior of as-prepared gelcast slurry. A premix solution was prepared with monomer/cross linker of AM/MBAM with ratio of 25:1. In this procedure, ammonium polyacrylate sodium (NHPANa) was used as the dispersant and the solid load included Al_2O_3/20 vol% ZrO_2 powder mixture. Series of slurries with different dispersant contents and solid loadings were prepared to investigate Shear-rate dependence behavior, using "Cross", "modified-Carreau" and "Carreau-Yasuda" models. Results further revealed that Carreau–Yasuda model with variant parameter 'a' proved the best fit on rheological behavior of gelcast slurries. Moreover, the results showed that the parameter 'a' for gel-cast slurries is around 3, which is much more than "Cross" and "modified-Carreau" models.

Keywords: Gelcast; Shear rate behavior; Carreau–Yasuda; Rheological modeling

1. Introduction

1.1. Gelcasting procedure

Gelcasting is a novel forming method for making complex-shaped ceramic bodies. The technique was first introduced by Young et al. [1] and then optimized by Janney et al. [2]. In this process, the prepared ceramic slurry is polymerized in situ after casting into a mold, producing a macromolecular network to hold the ceramic particles together. Distinct advantages of the gelcasting over the conventional ceramic forming are near-net-shape forming, high dried density, low levels of organic additives and machinability in the dried state owing to a high degree of homogeneity and high dried strength [3–10].

Although both non-aqueous and aqueous solvents can be used for gelcasting but aqueous system is preferred since this method is closer to traditional ceramic processing and has less environmental problems. In the aqueous gelcasting, acrylamide (AM) and methylen-bis-acrylamide (MBAM) are commonly used as monomer and cross-linker, respectively [11,12]. Composition of monomer solution, initiator amounts, catalyst additions, solid loading and humidity of drying atmosphere are important processing parameters for optimum gelcasting [7–12].

The present study attempts to focus on rheological behavior in order to determine the optimum condition for gel casting.

1.2. Shear rate dependence modeling

"Cross ", "Carreau" and "Carreau–Yasuda" are the most popular models to describe shear rate dependence of shear-thinning fluids with no yield point [13–18]. All these three models can be described in Eq. 1, which is derived from particles interactions in a dispersed system, such as polymer melts and solutions. All three of which are special cases of the following function form, explaining

*Corresponding author. Tel.: +98 21 6616 5263.
E-mail addresses: amirali.nojoomi@gmail.com, nojoomi@mehr.sharif.ir (A. Nojoomi).

0272-8842/$ - see front matter © 2013 Elsevier Ltd and Techna Group S.r.l. All rights reserved.
http://dx.doi.org/10.1016/j.ceramint.2013.05.112

particle interactions in a dispersed system.

$$\eta(\dot{\gamma}) = \eta_0[1 + (\lambda\dot{\gamma})^a]^{(n-1/a)} \quad (1)$$

η_0 is the viscosity of an initial Newtonian region at low shear rates for a shear-thinning fluid. At intermediate shear rate-s$\eta_0 \leq \eta \leq \eta_\infty$Eq. (1) yields an approximation to power-law behavior ($\sigma = K\gamma^n$) in which the exponent n is related to polydispersity. Increasing polydispersity tends to increase the value of n and consequently the gradient, $dlog\eta/dlog\eta_0$, at the intermediate shear-thinning region. The parameter "a" is the transition width parameter, which characterizes the breadth of transition between Newtonian and power-law regime. Narrow molecular weight distribution exhibits narrower breadth of transition and larger amount of "a".

The parameter λ is constant with unit of time, expressing a characteristic time corresponding with the terminal relaxation time, which can be defined by the ratioη_0/τ^* [13–16]. τ^*describes shear stress level at which η is in a transition from initial Newtonian region with viscosity η_0 to an intermediate shear-thinning region with power-law behavior. This is further clarified by Heiber [16], as it is shown in the following equation at $\dot{\gamma} = \tau^*/\eta_0$:

$$\eta = \eta_0(1/2)^{(n-1/a)} \quad (2)$$

The Models of "Cross" and "modified-Carreau" [16–18] correspond to Eq. (1) by $a = 1-n$ and $a = 1$, respectively. On the other hand, "Carreau–Yasuda" model considers 'a' free to be varied [19]. In this paper we propose a model that can explain shear rate dependence behavior of gelcast slurries through varying dispersant content and solid loading.

2. Raw materials and experimental procedure

2.1. Raw materials

α-Al_2O_3 powder (Alfa Aesar 99.99% with the particle size of 0.9–2.2 μm) and Zirconia powder (Aldrich 99% with the particle size of 5 μm) were used. Moreover, deionized water, acrylamide (AM) as monomer, methylene-bis-acrylamide (MBAM) as cross-linker, ammonium polyacrylate sodium as dispersant, and Poly ethylene glycol(PEG) as liquid desiccant were also used.

2.2. Experimental procedure

The premixed solution was prepared by dissolving 15 wt% monomer and cross-linker in distilled water. The weight ratio of monomer to cross-linker was 25:1. Then Alumina and Zirconia powders were added to the solution and the suspension was mixed for 60 min via ball milling. In order to investigate the effect of solid loading and dispersant content, different slurries were made with various solid loads of 40, 45, 48, 50 vol% as well as different dispersant contents of 0.3, 0.6, 0.9, and 1.2 wt% (on solid load weight basis). After complete mixing and de-airing, 0.15 wt% initiator and catalyst were added to the suspension to initiate the gelation.

Rheological behavior of as-prepared suspensions were investigated using Modular Compact rheometer (MCR300) at 25 °C, with a Cone–Plate measuring geometry (CP 25-2) having radius of 12.5 mm. Steady shear viscosity measurements were performed at various shear rates from 0.01 s^{-1} to 1000 s^{-1}. Finally, the model fitted by MATLAB programing.

3. Results and discussions

3.1. Experimental results

The mean particle size of the solid load after ball milling estimated at 0.1–0.2 μm for Alumina and 0.3–0.8 μm for zirconia powders. The data obtained from steady shear viscosity measurements for samples with different contents of dispersant are presented in Fig. 1.

The first part of the figure shows the initial Newtonian region at low shear rates. The second part represents the subsequent intermediate shear-thinning region that corresponds

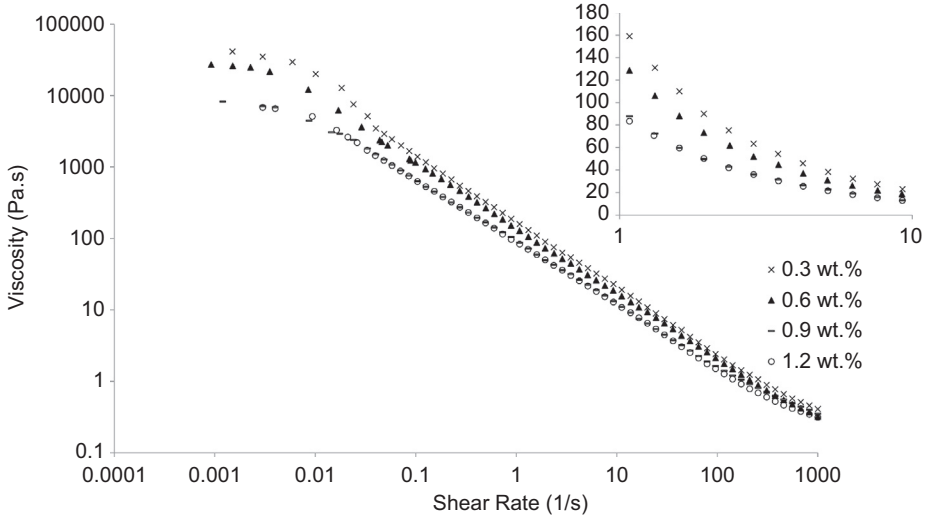

Fig. 1. Viscosity vs. shear-rate behavior of gel cast slurries with different contents of dispersant.

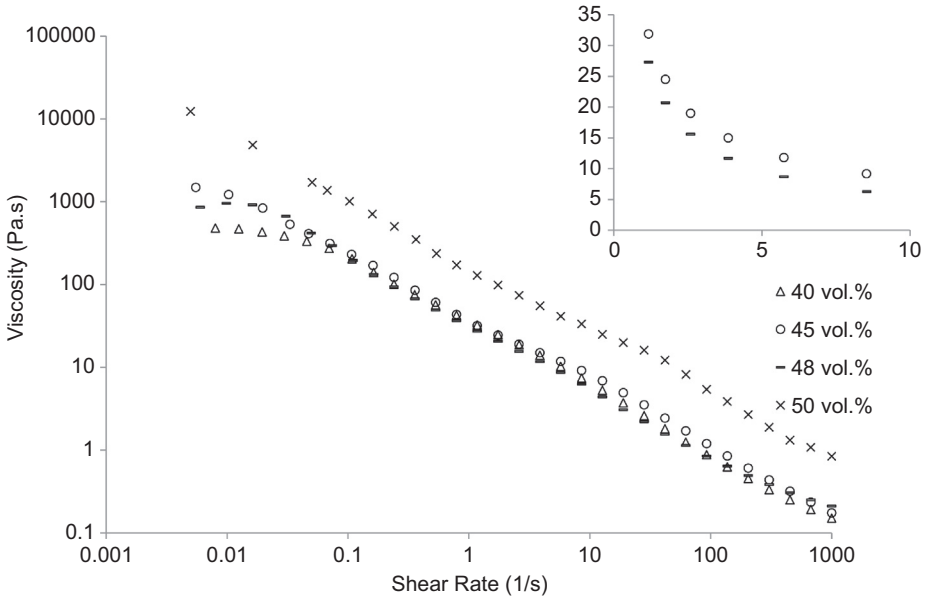

Fig. 2. Viscosity vs. shear-rate behavior of gel cast slurries with different contents of solid-loading.

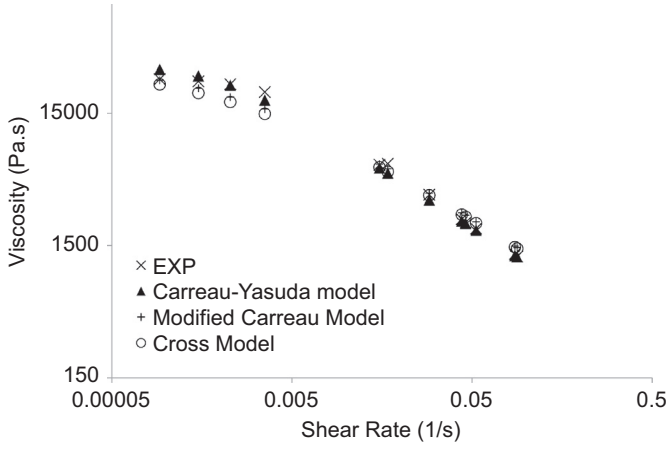

Fig. 3. Viscosity vs. shear-rate behavior of the slurry with 45 vol% solid loading and 0.6 wt% dispersant content for low shear-rate range, (a) Initial Newtonian region at low shear rates and (b) Following power law behavior.

to power-law relation. This figure also shows that when shear rates stays constant, by increasing dispersant content viscosity tends to decrease.

Powder aggregation and creation of 'soft' agglomerates are the results of the attractive van der Waals forces in water based suspension mediums. There are three main routes by which an unstable colloidal suspension can become a stable and dispersed system: (1) electrostatic dispersion, (2) steric dispersion and (3) electro–steric dispersion. Electro–steric dispersion involves the adsorption of charged polymers known as polyelectrolytes on an electrostatically charged surface of powders. Complete dispersion will achieve when sufficient dispersant is adsorbed on the particle surface. This phenomenon creates a Debye length that exceeds the scope of van der Waals forces. Thus, the configuration of the dispersant chains (NHPANa) on the surface of ceramic powder can significantly affect the dispersion degree of the colloidal system in constant dispersant content.

Ammonium poly-acrylate, with weak acid groups such as carboxylic acid, is classified as a 'weak' polyelectrolyte, which is sensitive to pH changes of the suspension. Since our investigation was performed under intrinsic pH of 9–9.5, both polymer and powder have negative charges [20]. This negative charge makes the linear polyelectrolyte to suspend in solution while adsorbs to powder surface only at the few minor regions of positive surface charge. These positive sites are created by the absorption of counter-ions to the negative sites of the powder surface, which subsequently decreases the surface charge.

Considering dispersants were chosen in the second viscosity minima as recommended by Davies [20](more than 3 mgr. per gr of powder), there were enough regions of positive surface charge due to the presence of counter-ions. High concentration of counter ions assists loop formation and congregation of NHPANa chains on the powder surface. This can cause the extension of polymer chains in the solution, producing a steric barrier. Steric barrier coupled with electrostatic barrier provides an electro–steric repulsive force that exceeds Van der Waals attractive forces and increases the dispersion degree. Davies [20] indicated that the decrease in viscosity corresponds to development of the loop and tail configurations of the dispersant, which is attached to the surface of the powder.

The concentration of counter-ions is proportional to the concentration of NHPANa. Thus, the number of positively charged reigns on the powder surface, where NHPANa polymers are attached, increases by increasing the concentration of dispersant. Therefore, it cab be inferred that higher

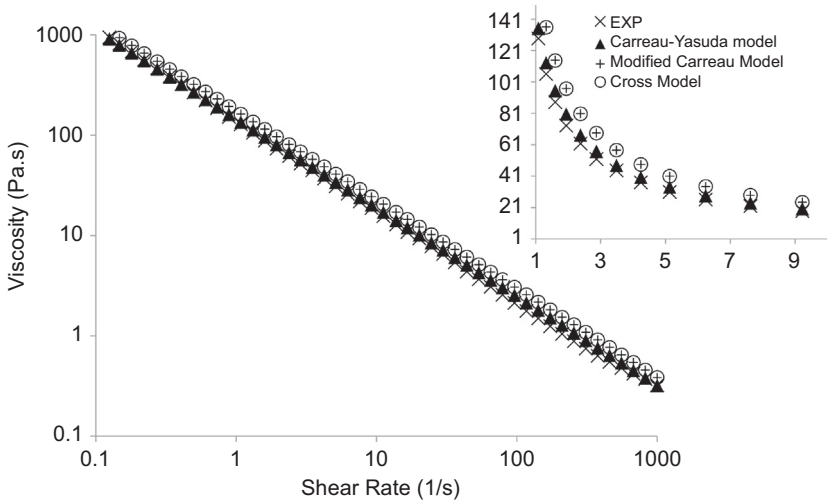

Fig. 4. Viscosity vs. shear-rate behavior and fitted models of the slurry with 45 vol% solid loading and 0.6 wt% dispersant content for high shear-rates.

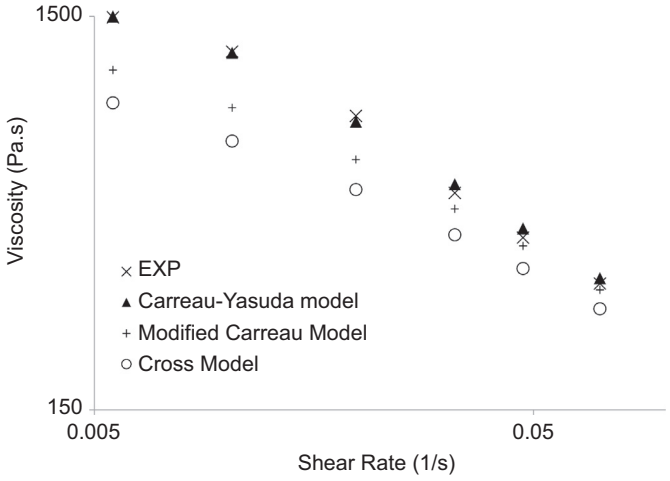

Fig. 5. Viscosity vs. shear-rate behavior of the slurry with 48 vol% solid loading and 0.6 wt% dispersant content for low shear rates, (a) Initial Newtonian region at low shear rates and (b) following power law behavior.

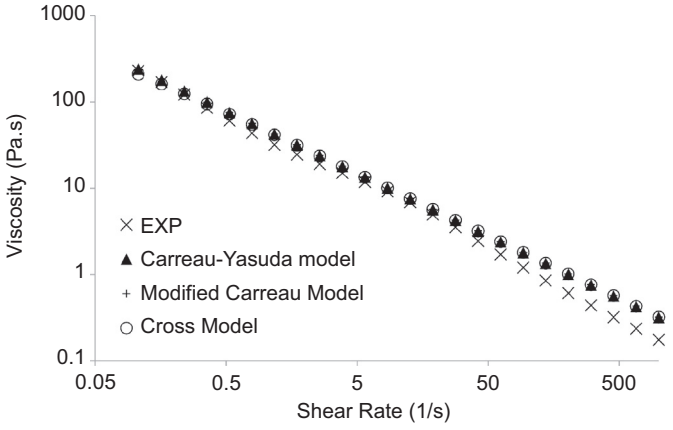

Fig. 6. Viscosity vs. shear rate behavior and fitted models of the slurry with 48 vol% solid loading and 0.6 wt% dispersant content for high shear rates.

amounts of dispersant results in lower viscosity at low shear rates (η_0) (Fig. 1).

At high shear rates, conformation of attached NHPANa changes continuously and severely. Thus, the steric barrier becomes thinner and consequently viscosity dependence to the dispersant content declines. Therefore, as shear rate increases, the viscosity divergence among different samples decreases.

Viscosity as a function of solid loading with 0.6 wt% dispersant content is shown in Fig. 2. All slurries demonstrate the same pseudoplastic flow behavior. Viscosity of the slurry with 50 vol% ceramic content is considerably higher than those of other slurries, due to excessive solid loading.

Watanabe [20] claims that the best dispersion is achieved when steric barrier provided by polymer chains coupled with the electrostatic layer, delivers an electro–steric repulsive barrier. By increasing the solid loading, the amount of dispersant, which is needed to obtain an appropriate steric barrier tend to rise. Thus, at high solid loading levels appropriate dispersion becomes impossible. This can be seen in 50 vol% solid loading curve, showing no appropriate rheological behavior to be casted.

3.2. Viscosity fitting

In the following section, we will discuss the best behavior model of gel-cast slurries so that it can be used in molding process simulations. In this regard, Eq. (1) is applied to the derived data from steady shear viscosity measurements in interval of 0.01–1000 s^{-1}. Experimental data of the viscosity against solid loading and dispersant content is shown in Fig. 1. For each data, three fits were found using Eq. 1. Parameter '*a*' is considered "variant" for Carreau–Yasuda model, "1" for modified Carreau and "1−n" for Cross model.

Experimental data along with the fitted curves for the slurry with 0.6 wt% dispersant and 45 vol% solid loading are shown in Fig. 3 and 4. Viscosity-shear rate behavior of the slurry for

low shear rates along with fitted curves is represented in Fig. 3. The initial Newtonian region at low shear rates (Fig. 3a), and the transition to subsequent power-law behavior (Fig. 3b), has been demonstrated for experimental data.

The experimental data was extrapolated to zero shear rate to discover the viscosity of an initial Newtonian region (η_0). As noted earlier, λ was defined by shear stress level at which η is in transition from initial Newtonian region to an intermediate shear-thinning region. λ can further be determined separately from transition region of each experimental data set (e.g. transition form Fig. 3a and b). Finally, parameter 'n' is driven from subsequent power-law behavior of each experimental data set. So 'a' is a key parameter to determine the adjustment degree of the fitting curve.

Among all three models, Carreau–Yasuda model, with 'a' around 3, yields the best fit with adjustment of 0.9924. Also, Carreau–Yasuda model has successfully managed to show the transition behavior of the slurry. For shear rates above 1 s^{-1} at which the behavior exactly obeys power-law, indicates that all three models fit properly (Fig. 4).

This conclusion can be applied to data of 48 vol% solid loading with 0.6 wt% dispersant as shown in Figs. 5 and 6.

Data of η_0, which were obtained with the best-fitted models, confirmed that the amount of η_0 decreases by dispersant increment (Table 1).

As it is clear, "Carreau–Yasuda" gives the best fit due to the variability of 'a'. Moreover, the amount of 'n' is lower than that of for polymer melts or solutions, which was lied in the interval of 0.2–0.4 [16–18]. This can be explained by the use of mono-dispersed monomers in premix solution. Also, the amount of 'a' is determined to be at the vicinity of 3, which is more than "Carreau", "modified Carreau" and also "Cross" models [13–15]. This in turn shows narrower molecular weight distribution in comparison with other polymer-based slurries.

Tables 1 and 2 summarize the results of curve fitting. Parameters RMSE and ADJ R-square show the deviation and adjustment of each fitted curve, respectively.

The amounts of λ and η_0 are depended on the slurry's behavior and yet independent from models, while; 'a' and 'n' both are curve-fitting parameters.

Table 1
Fitting parameters for slurries with different dispersant contents at 48 vol% solid loading.

Dispersant content	Model	*a*	*n*	λ (s)	η_0 (Pa s)	ADJ R-square[a]	RMSE[b]
0.3 wt%	Cross	0.93	0.0674	177	23000	0.67	0.13
	Modified Carreau	1	0.0674	177	23000	0.7	0.13
	Carreau–Yasuda	3	0.0674	177	23000	0.9	0.07
0.6 wt%	Cross	0.89	0.114	440	30000	0.87	0.07
	Modified Carreau	1	0.114	440	30000	0.9	0.06
	Carreau–Yasuda	2.89	0.114	440	30000	0.9924	0.018
0.9 wt%	Cross	0.838	0.1624	186	7000	0.85	0.07
	Modified Carreau	1	0.1624	186	7000	0.9	0.05
	Carreau–Yasuda	2.35	0.1624	186	7000	0.974	0.03
1.2 wt%	Cross	0.865	0.1345	130	6000	0.083	0.06
	Modified Carreau	1	0.1345	130	6000	0.87	0.05
	Carreau–Yasuda	3	0.1345	130	6000	0.99	0.01

[a]Adjusted R-square.
[b]Root-mean-square-error.

Table 2
Fitting parameters for slurries with different solid loadings contents at 0.6 wt% dispersant content.

Solid loading		*a*	*n*	λ (s)	η_0 (Pa.s)	ADJ R-square[a]	RMSE[b]
40 vol%	Cross	0.7474	0.2731	45	500	0.8	0.15
	Modified Carreau	1	0.2723	45	500	0.9	0.1
	Carreau–Yasuda	3.08	0.2755	45	500	0.9885	0.03
45 vol%	Cross	0.7676	0.2324	89	1000	0.73	0.15
	Modified Carreau	1	0.2324	89	1000	0.84	0.12
	Carreau–Yasuda	3.95	0.2324	89	1000	0.97	0.06
48 vol%	Cross	0.7246	0.2755	128	1600	0.8196	0.0987
	Modified Carreau	1	0.2755	128	1600	0.922	0.064
	Carreau–Yasuda	3.2	0.2755	128	1600	0.9991	0.007

[a]Adjusted R-square.
[b]Root-mean-square-error.

Since all models have predicted power-law region, the parameter '*n*' is the same for all models at each dataset.

4. Conclusion

Based upon the obtained data from rheological behavior, it can be concluded that gel cast suspensions demonstrate behavior analogous to that of polymer melts and solutions, in that they all exhibit initial Newtonian region at law shear rates. Furthermore they show subsequent intermediate shear thinning corresponding to the power-law relation.

The role of dispersant content and solid loading on the behavior of suspension was investigated. Results revealed that by increasing the dispersant content, electro–steric repulsive barrier leads to better dispersion. It seems that after a particular amount of dispersant content, in which two mechanisms of dispersions are available, further dispersant cannot be helpful. However, excessive solid loading showed a jump on viscosity.

Viscosity fitting shows that all models can appropriately predict power-law behavior, whereas, Carreau–Yasuda model with variable parameter of '*a*' yields the best result showing both Newtonian and power-law region with adjustment higher than 0.97. Unlike previous reports on polymer melt modeling, we obtained lower amount of '*n*', which lies around 0.05–0.3 interval. The results further revealed that the amount of '*a*' reached close to 3. Thus, it is recommended that in order to reduce the required computer execution time, the parameter '*a*' should be kept at 3.

Acknowledgment

This research was supported by Iranian National Science Foundation (INSF). We would like to thank Mr. Cina Aghammohadi (Electrical Engineering Department, Sharif University of Technology) for his assistance in fitting curve algorithms. We also like to thank Dr. Kiumars Zarafshani from Razi University for reviewing the final draft.

References

[1] A.C. Young, O.O. Omatete, M.A. Janney, P.A. Menchhofe, Gelcasting of Alumina, Journal of American Ceramic Society 74 (3) (1991) 612–618.
[2] M.A. Janney, O.O. Omatete, C.A. Walls, S.D. Nunn, R.J. Ogle, G. Westmoreland, Development of low-toxicity gelcasting systems, Journal of American Ceramic Society 81 (3) (1998) 581–591.
[3] J.A. Lewis, Colloidal processing of ceramics, Journal of American Ceramic Society 83 (10) (2000) 2341–2359.
[4] A.G. King, Ceramic technology and processing", 10th Printing, Noyes/William Andrew Publications, USA, 2002.
[5] Sh.L. Morissette, J.A. Lewis, Chemorheology of aqueous-based alumina–poly(vinyl alcohol) gelcasting suspensions, Journal of American Ceramic Society 82 (3) (1999) 521–528.
[6] K. Cai, Y. Huang, J. Yang, A synergistic low-toxicity gelcasting system by using HEMA and PVP, Journal of American Ceramic Society 88 (12) (2005) 3332–3337.
[7] A.C. Young, O.O. Omatete, M.A. Janney, Paul A Menchhofer, . Gelcasting of alumina, Journal of American Ceramic Society 74 (4) (2005).
[8] L.M. Sheppard, Gelcasting enters the fast lane, Ceramic Industry 150 (4) (2000) 26.
[9] G. Tari, Gelcasting ceramics: a review, American Ceramic Society Bulletin 82 (4) (2003) 43.
[10] Q. Zhang, M. Gu, Rheological properties and gelcasting of concentrated aqueous silicon suspension, Materials Science and Engineering A 399 (2005) 351–357.
[11] Ali Akbar Kokabi, Ali Akbar Babaluo, Abolfazl Barati, Gelation process in low-toxic gelcasting systems, Journal of the European Ceramic Society 26 (2006) 3083–3090.
[12] J. Maa, Z. Xiea, H. Miaoa, Y. Huanga, Y. Chengb, Gelcasting of ceramic suspension in acrylamide/polyethylene glycol systems, Ceramics International 28 (2002) 859–864.
[13] M.M. Cross, A. Kaye, Simple procedures for obtaining viscosity/shear rate data from a parallel disc viscometer, Polymer 28 (1987) 435–440.
[14] M.M. Cross, Relation between viscoelasticity and shear-thinning behavior in liquids 18 (1979) 609–614.
[15] M.M. Cross, Analysis of flow data on molten polymers, European Polymer Journal 2 (1966) 299–307.
[16] C.A. Hieber, H.H. Chang, Shear rate dependence modeling of polymer melt viscosity, Polymer Engineering Science 32 (1992) 931–938.
[17] H. Watanabe, Viscoelasticity and dynamics of entangled polymers, Progress in Polymer Science 24 (1999) 1253–1403.
[18] N. Fatkullin, C. Mattea, S. Stapf, A simple scaling derivation of the shear thinning power-law exponent in entangled polymer melts, Polymer 52 (2011) 3522–3525.
[19] H. Kühnle, Evaluation of the viscoelastic temperature and pressure shift factor over the full range of shear rates, Parts I and II, International Polymer Processing 1 (1987) 89–97, pp. 116–122.
[20] J. Davies 1, J.G.P. Binner, The role of ammonium polyacrylate in dispersing concentrated alumina suspensions, The role of ammonium polyacrylate in dispersing concentrated alumina suspensions, Journal of The European Ceramic Society 20 (2000) 1539–1553.